Journal of Thermal Analysis and Calorimetry, Vol. 65 (2001) 805–819

COMPARATIVE THERMODYNAMIC INVESTIGATION OF THE Bi–GaSb SYSTEM

D. ivković[*]*, . ivković, L. Stuparević and S. Rančić*

University of Belgrade, Technical Faculty, Department of Metallurgy, VJ 12, 19210 Bor,
Yugoslavia

(Received July 17, 2000; in revised form February 20, 2001)

Abstract

Results of the thermodynamic investigations in the Bi–GaSb system are presented in this paper. Thermodynamic characteristics experimentally determined by Oelsen's calorimetric method were compared with values predicted by different thermodynamic predicting methods (general solution model, Kohler, Muggianu, Toop, Hillert) at the temperature of 1073 K. Also, based on the obtained cooling curves and microstructure analysis of the investigated samples by optical microscopy, phase diagram of the Bi–GaSb system was investigated and compared with literature data.

Keywords: alloy thermodynamics, calorimetry, thermodynamic predicting method, ternary system Bi–GaSb

Introduction

Among many different alloy systems containing semiconducting compounds, GaSb-based materials have been the subject of an increasing attention in the semiconductor production [1–6]. One of these systems, which has an important industrial application in the solid state electronic devices, is the ternary system Bi–Ga–Sb [1].

Many studies have been carried out in order to obtain accurate data on the thermodynamic properties and phase diagram of this system [7–24]. But, although there are a lot of references concerning the thermodynamics of the constituent binary systems Ga–Sb [7–13], Bi–Sb [14–17] and Ga–Bi [1, 18–21], there are only a few thermodynamic data for the ternary Bi–GaSb system [1, 22, 23]. So, in the work of Katayama and co-workers [1], who performed the emf measurement of the electrochemical cell with zirconia as solid electrolyte, gallium activities at 1073 K were obtained for selected alloy compositions. Also, predicting of gallium thermodynamic quantities in five sections of this system at a temperature of 1073 K is given in the work of ivković *et al.* [22], while the same authors recently presented the results of

---

[*] Author for correspondence: Phone/Fax: ++381 30 424 547; E-mail: jmm@eunet.yu

1418–2874/2001/ $ 5.00

Akadémiai Kiadó, Budapest
Kluwer Academic Publishers, Dordrecht

experimental investigations done by calorimetry, DTA and SEM for the system Bi–$Ga_{0.1}Sb_{0.9}$ [23].

In order to complete the thermodynamic data and enable the further interpretation of the phenomena occurring in Bi–GaSb alloys, the results of comparative thermodynamic analysis and phase diagram investigation of the Bi–GaSb system, are presented in this paper.

Experimental

Oelsen's calorimetry was used for the experimental thermodynamic analysis of the investigated system. Description of that experimental technique can be found in [24–26].

The water equivalent was determined by a standard method using dissolved Na_2CO_3, and for the calorimeter used it has a value of 2705 J K^{-1}. All experiments were performed with pure bismuth, gallium and antimony of p.a. grade, in air atmosphere.

The calorimetric measurements and thermodynamic calculations in the Bi–GaSb system were carried out along the line of a constant mole ratio Ga:Sb=1:1, as is indicated in Fig. 1. The composition and masses of ten samples investigated are given in Table 1.

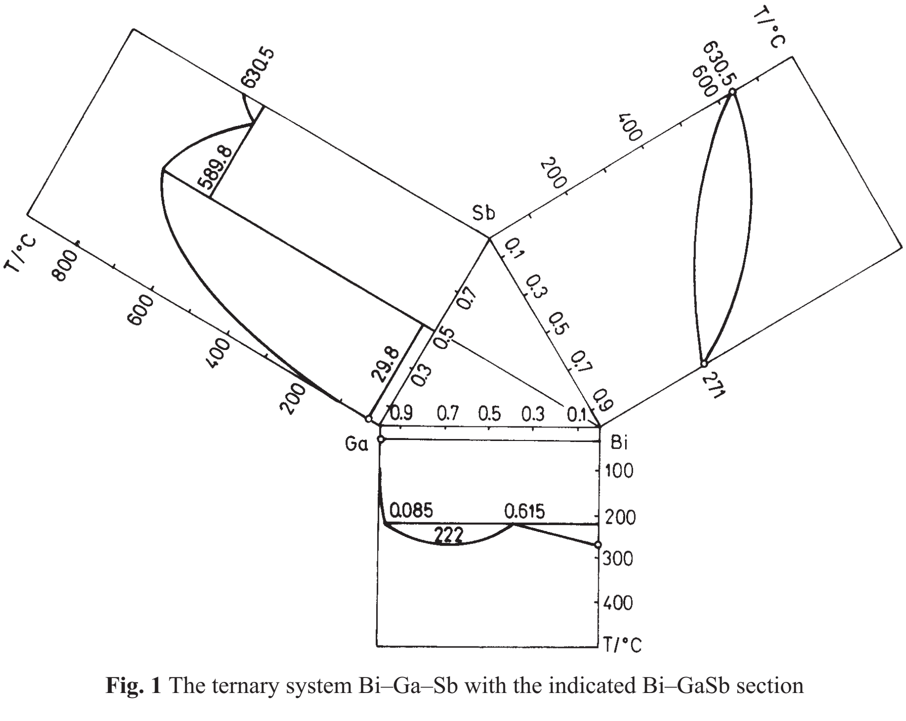

Fig. 1 The ternary system Bi–Ga–Sb with the indicated Bi–GaSb section

Table 1 Composition and masses of the investigated samples

Alloy	Molar content			Composition/mass%			*m*/g		
	Bi	Ga	Sb	Bi	Ga	Sb	Bi	Ga	Sb
L0	1	0	0	100	0	0	9.800	0	0
L1	0.98	0.01	0.01	99.074	0.589	0.337	9.661	0.033	0.057
L2	0.90	0.05	0.05	95.157	3.080	1.763	9.088	0.168	0.294
L3	0.70	0.15	0.15	83.589	10.435	5.975	7.528	0.538	0.940
L4	0.50	0.25	0.25	68.583	19.978	11.439	5.751	0.959	1.675
L5	0.30	0.35	0.35	48.336	32.853	18.812	3.709	1.443	2.521
L6	0.10	0.45	0.45	19.521	51.176	29.303	1.336	2.005	3.502
L7	0	0.50	0.50	0	63.589	36.411	0	2.322	4.055

Microstructure of the investigated samples was examined by optical microscopy, using a Reichert MeF2 microscope.

Theoretical fundamentals

Oelsen calorimetry

Concerning the alloy of the composition $x_B=x$ at the temperature T in the binary eutectic system A–B, the integral Gibbs energy of mixing is given as

$$\Delta G^{M}_{x,T}=(1-x)G^{M}_{A,T}+xG^{M}_{B,T}=(1-x)RT\ln a_{A,T}+xRT\ln a_{B,T} \tag{1}$$

or according to the Gibbs–Helmholtz equation

$$\Delta G^{M}_{x,T}=\Delta H^{M}_{x,T}-T\Delta S^{M}_{x,T}, \tag{2}$$

and the following expression is obtained

$$\Delta H^{M}_{x,T}-T\Delta S^{M}_{x,T}=(1-x)RT\ln a_{A,T}+xRT\ln a_{B,T} \tag{3}$$

In Oelsen thermodynamic analysis [24–26], thermodynamic properties are determined by the so-called Oelsen integral, which enables the calculation of the partial molar Gibbs energy of mixing from directly measured values of enthalpies. Further determination of the activation for the constituent components is conceived on the knowledge of the enthalpy and entropy terms. Under equilibrium conditions and constant pressure, the entropy term can be written as

$$\mathrm{d}S^{M}_{x,T}=\frac{\mathrm{d}H^{M}_{x,T}}{T} \tag{4}$$

and

$$S^{\mathrm{M}}_{\mathrm{x,T}} = S^{\mathrm{M}}_{\mathrm{x,T=0}} + \int_{\mathrm{H}^{\mathrm{M}}_{\mathrm{x,T=0}}}^{\mathrm{H}^{\mathrm{M}}_{\mathrm{x,T}}} \frac{\mathrm{d}H^{\mathrm{M}}_{\mathrm{x,T}}}{T} \tag{5}$$

and using the Nernst theorem, $S^{\mathrm{M}}_{\mathrm{x,T}}=0$, it follows that

$$S^{\mathrm{M}}_{\mathrm{x,T}} = \int_{\mathrm{H}^{\mathrm{M}}_{\mathrm{x,T=0}}}^{\mathrm{H}^{\mathrm{M}}_{\mathrm{x,T}}} \frac{\mathrm{d}H^{\mathrm{M}}_{\mathrm{x,T}}}{T} \tag{6}$$

Based on the Eqs (3) and (6), one could obtain

$$\Delta G^{\mathrm{M}}_{\mathrm{x,T}} = H^{\mathrm{M}}_{\mathrm{x,T}} - T\int_{\mathrm{H}^{\mathrm{M}}_{\mathrm{x,T=0}}}^{\mathrm{H}^{\mathrm{M}}_{\mathrm{x,T}}} \frac{\mathrm{d}H^{\mathrm{M}}_{\mathrm{x,T}}}{T} \tag{7}$$

For a better survey, Oelsen introduced the quantity, $I_{\mathrm{x,T}}$, which represents the value of the enthalpy, directly determined in a calorimeter:

$$I_{\mathrm{x,T}} = H^{\mathrm{M}}_{\mathrm{x,T}} - H^{\mathrm{M}}_{\mathrm{x,V}} \tag{8}$$

where V is the room temperature of 298 K. Multiplying Eq. (7) with $(-T)$ and using Eq. (8), it follows

$$-G^{\mathrm{M}}_{\mathrm{x,T}} = \int_{\mathrm{I}_{\mathrm{x,T=0}}}^{\mathrm{I}_{\mathrm{x,T}}} \frac{\mathrm{d}I^{\mathrm{M}}_{\mathrm{x,T}}}{T} - \int_{1/\mathrm{V}}^{1/\mathrm{T}} I_{\mathrm{x,T}}\,\mathrm{d}\left(\frac{1}{T}\right) \tag{9}$$

which represent the important Oelsen integral. The solution of this integral is done by a graphical planimetry of the area below the cooling curve.

Therefore, the basic equation of the Oelsen quantitative thermodynamic analysis [24–26] is

$$-G^{\mathrm{M}}_{\mathrm{i}} = \int_{1/\mathrm{T}_0}^{1/\mathrm{T}} H_{\mathrm{x,T}}\,\mathrm{d}\left(\frac{1}{T}\right) = -R\ln a_{\mathrm{i}} \tag{10}$$

where are $G^{\mathrm{M}}_{\mathrm{i}}$ – the partial Gibbs energy of mixing for the component i, T_0 – the starting temperature, T – the finite temperature, $H_{\mathrm{x,T}}$ – the enthalpy value measured in the Oelsen calorimeter for the temperature change from T_0 to T, R – the gas constant, and a_{i} – the activity of the component i.

It should be stated that Oelsen calorimetric method could also be used for the thermodynamic analysis of quasibinary systems of simple eutectic type [27].

Thermodynamic predicting methods

According to Hillert [28], traditional thermodynamic predicting methods are classified into two categories: symmetrical (Kohler, Muggianu) and asymmetrical (Toop, Hillert). There is also a recently provided general solution model (Chou) [29], which breaks down the boundary between symmetrical and asymmetrical models, and has already been proved in some practical examples [29–31] as the correct and accurate method.

The basic theoretical interpretations of these methods are given:

Kohler model [32]

$$G^{\mathrm{E}}=(x_1+x_2)^2\Delta G_{12}^{\mathrm{E}}\left(\frac{x_1}{x_1+x_2};\frac{x_2}{x_1+x_2}\right)+(x_2+x_3)^2\Delta G_{23}^{\mathrm{E}}\left(\frac{x_2}{x_2+x_3};\frac{x_3}{x_2+x_3}\right)+ \\ +(x_3+x_1)^2\Delta G_{31}^{\mathrm{E}}\left(\frac{x_3}{x_1+x_3};\frac{x_1}{x_1+x_3}\right) \tag{11}$$

Muggianu model [33]

$$G^{\mathrm{E}}=\frac{4x_1x_2}{(1+x_1-x_2)(1+x_2-x_1)}\Delta G_{12}^{\mathrm{E}}\left(\frac{1+x_1-x_2}{2};\frac{1+x_2-x_1}{2}\right)+ \\ +\frac{4x_2x_3}{(1+x_2-x_3)(1+x_3-x_2)}\Delta G_{23}^{\mathrm{E}}\left(\frac{1+x_2-x_3}{2};\frac{1+x_3-x_2}{2}\right)+ \\ +\frac{4x_3x_1}{(1+x_3-x_1)(1+x_1-x_3)}\Delta G_{31}^{\mathrm{E}}\left(\frac{1+x_3-x_1}{2};\frac{1+x_1-x_3}{2}\right) \tag{12}$$

Toop model [34]

$$G^{\mathrm{E}}=\frac{x_2}{1-x_1}\Delta G_{12}^{\mathrm{E}}(x_1;1-x_1)+\frac{x_3}{1-x_1}\Delta G_{13}^{\mathrm{E}}(x_1;1-x_1)+ \\ +(x_2+x_3)^2\Delta G_{23}^{\mathrm{E}}\left(\frac{x_2}{x_2+x_3};\frac{x_3}{x_2+x_3}\right) \tag{13}$$

Hillert model [28]

$$G^{\mathrm{E}}=\frac{x_2}{1-x_1}\Delta G_{12}^{\mathrm{E}}(x_1;1-x_1)+\frac{x_3}{1-x_1}\Delta G_{13}^{\mathrm{E}}(x_1;1-x_1)+ \\ +\frac{x_2x_3}{v_{23}v_{32}}\Delta G_{23}^{\mathrm{E}}(v_{23};v_{32}) \tag{14}$$

where $v_{\mathrm{ij}}=1/2(1+x_{\mathrm{i}}-x_{\mathrm{j}})$.

Chou model [29]

$$G^{\mathrm{E}}=x_1x_2[A_{12}^0+A_{12}^1(x_1-x_2)+A_{12}^2(x_1-x_2)^2]+ \\ +x_2x_3[A_{23}^0+A_{23}^1(x_2-x_3)+A_{23}^2(x_2-x_3)^2]+ \\ +x_3x_1[A_{31}^0+A_{31}^1(x_3-x_1)+A_{31}^2(x_3-x_1)^2]+fx_1x_2x_3 \tag{15}$$

where $A^0_{ij}, A^1_{ij}, A^2_{ij}$ are parameters for binary system '*ij*' independent of composition, only relying on temperature, which have been used in the regular type equation:

$$G^E_{ij} = X_i X_j [A^0_{ij} + A^1_{ij}(X_i - X_j) + A^2_{ij}(X_i - X_j)^2 + \ldots + A^n_{ij}(X_i - X_j)^2] \tag{16}$$

where X_i and X_j indicate the mole fraction of component '*i*' and '*j*' in '*ij*' binary system. The function *f* is the ternary interaction coefficient expressed by

$$\begin{aligned} f = {} & (2\xi_{12} - 1)\{A^2_{12}[(2\xi_{12} - 1)x_3 + 2(x_1 - x_2)] + A^1_{12}\} + \\ & + (2\xi_{23} - 1)\{A^2_{23}[(2\xi_{23} - 1)x_1 + 2(x_2 - x_3)] + A^1_{23}\} + \\ & + (2\xi_{31} - 1)\{A^2_{31}[(2\xi_{31} - 1)x_2 + 2(x_3 - x_1)] + A^1_{31}\} \end{aligned} \tag{17}$$

where ξ_{ij} are the similarity coefficients defined by η_i called the deviation sum of squares:

$$\xi_{ij} = \frac{\eta_i}{\eta_i + \eta_j} \tag{18}$$

where

$$\begin{aligned} \eta_I &= \int_{X_i=0}^{X_i=1} (\Delta G^E_{12} - \Delta G^E_{13})^2 \mathrm{d}X_1 \\ \eta_{II} &= \int_{X_i=0}^{X_i=1} (\Delta G^E_{21} - \Delta G^E_{23})^2 \mathrm{d}X_2 \\ \eta_{III} &= \int_{X_i=0}^{X_i=1} (\Delta G^E_{31} - \Delta G^E_{32})^2 \mathrm{d}X_3 \end{aligned} \tag{19}$$

and

$$\begin{aligned} X_{1(12)} &= x_1 + x_3\xi_{12} \\ X_{2(23)} &= x_2 + x_1\xi_{23} \\ X_{3(31)} &= x_3 + x_2\xi_{31} \end{aligned} \tag{20}$$

In all given equations, G^E and G^E_{ij} correspond to the integral model excess Gibbs energies for ternary and binary systems, respectively, while x_1, x_2, x_3 correspond to the mole fraction of components in investigated ternary system.

Results and discussion

First of all, the phase diagram of the Bi–GaSb system was investigated based on the cooling curves obtained by the Oelsen's calorimetry and the results of microstructure analysis. Its graphical representation, compared with the literature data [35], is given in Fig. 2, while the characteristic microphotographs, obtained by the optical microscopy, are shown in Fig. 3.

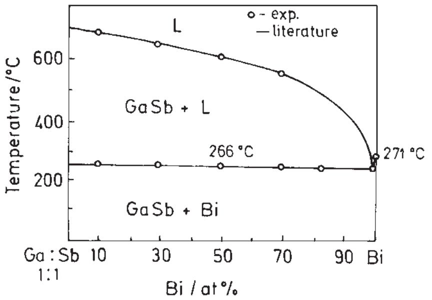

Fig. 2 Phase diagram of the Bi–GaSb system

Eutectic type of the phase diagram is noticed, with the eutectic reaction at the temperature of 539 K and the eutectic point appearing at 98 at%Bi. The quasibinary hypoeutectic alloys (samples L2–L6) are presented in the widest part of the investigated concentration range in the Bi–GaSb system, and solidify with the primary crys-

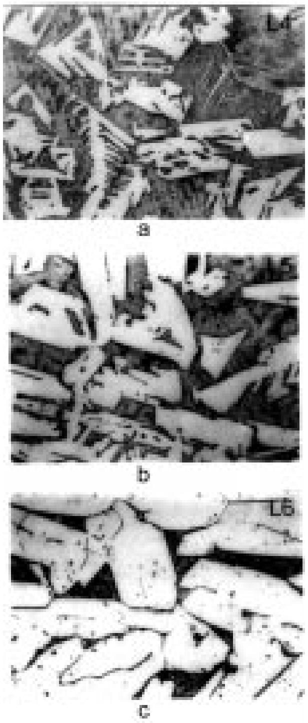

Fig. 3 Characteristic microphotographs for samples: a – L4; b – L5; c – L6 (light phase – primary solidified GaSb crystals; dark phase – binary eutectics (GaSb+Bi)

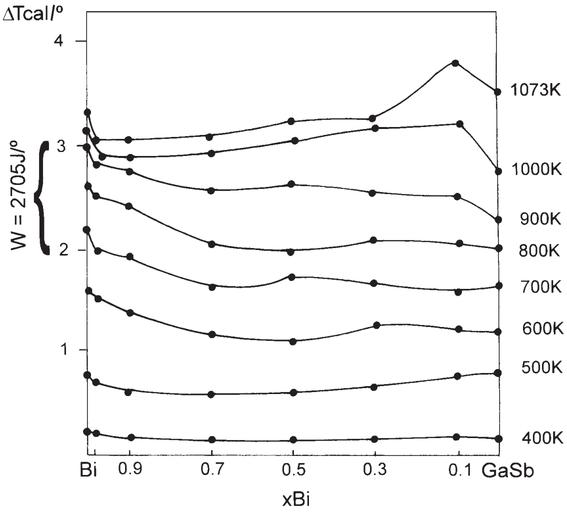

Fig. 4 The enthalpy isotherm diagram for the temperature interval 400–1073 K

tallization of the intermetallic compound GaSb and the eutectic reaction (GaSb+Bi). As can be seen from the microstructures in Fig. 3, the quantity of the primarily solidified GaSb crystals (light phase) increases by the bismuth concentration decreasing. This phase has an oriented crystallization and forms characteristic geometrical shapes with the presented dendrites of the ‘chinese letters’ type.

Further, based on the cooling curves obtained by Oelsen’s calorimetry, temperature changes of the used calorimeter were determined for all samples in the investigated temperature interval 400–1073 K. According to these data, dependence of the calorimeter temperature change on composition, called the enthalpy isotherm diagram, was constructed and presented in Fig. 4.

Further step in the Oelsen’s quantitative analysis is the graphic planimetry, as shown in Fig. 5, while the final part of the calculation – construction of the tangent

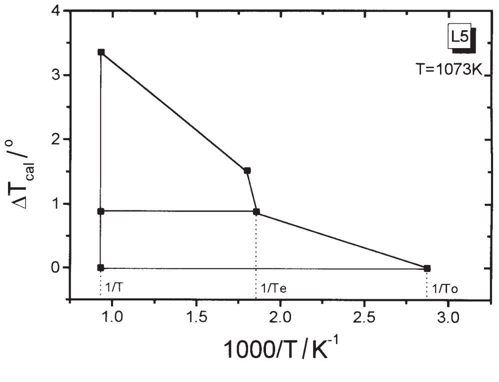

Fig. 5 Graphic planimetry (for the sample L5)

for the determination of $-R\ln a_{\mathrm{Bi}}$ at different temperatures, is done according to Eq. (10), and given in Fig. 6.

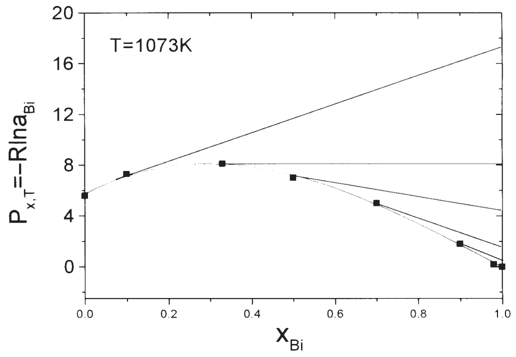

Fig. 6 Construction of the tangent for the determination of $-R\ln a_{\mathrm{Bi}}$ (at 1073 K)

Review of the results obtained by Oelsen's quantitative thermodynamic analysis, which includes activities, activity coefficients and partial molar quantities for bismuth in the investigated composition range at temperatures 973, 1023, 1073 K, is given in Table 2.

Table 2 Results of the Oelsen's quantitative thermodynamic analysis

T/K	x_{Bi}	a_{Bi}	γ_{Bi}	$G^{\mathrm{M}}_{\mathrm{Bi}}$/ J mol^{-1}	$G^{\mathrm{E}}_{\mathrm{Bi}}$/ J mol^{-1}
973	1	1	1	0	0
	0.98	0.994	1.014	–49	91
	0.9	0.938	1.042	–518	266
	0.7	0.789	1.127	–1917	769
	0.5	0.631	1.262	–3725	1495
	0.3	0.422	1.407	–6979	2193
	0.1	0.149	1.49	–15401	2563
1023	1	1	1	0	0
	0.98	0.991	1.011	–77	95
	0.9	0.931	1.034	–608	288
	0.7	0.764	1.091	–2289	744
	0.5	0.618	1.236	–4093	1802
	0.3	0.397	1.323	–7857	2383
	0.1	0.132	1.32	–17223	2361
1073	1	1	1	0	0
	0.98	0.988	1.008	–108	73
	0.9	0.927	1.030	–676	264
	0.7	0.755	1.079	–2507	675
	0.5	0.601	1.202	–4542	1641
	0.3	0.382	1.273	–8585	2156
	0.1	0.124	1.240	–18622	1919

Positive deviation from the Raoult's law can be noticed for bismuth activities in all investigated samples at given temperatures, which causes the positive values for the partial molar excess Gibbs energies. This indicates somehow a slight immiscibility, characteristic of the behavior of bismuth. Having in mind the phase diagram of Bi–GaSb system (Fig. 2), it is clear that the interactions between gallium and antimony, which form the intermetallic compound, are much stronger, comparing to the interactions between bismuth and other two components. Also, it should be stated, that slight deviation from the ideal solution behavior is noticed in this case, as was already confirmed in literature [1, 22] for the whole ternary Bi–GaSb system.

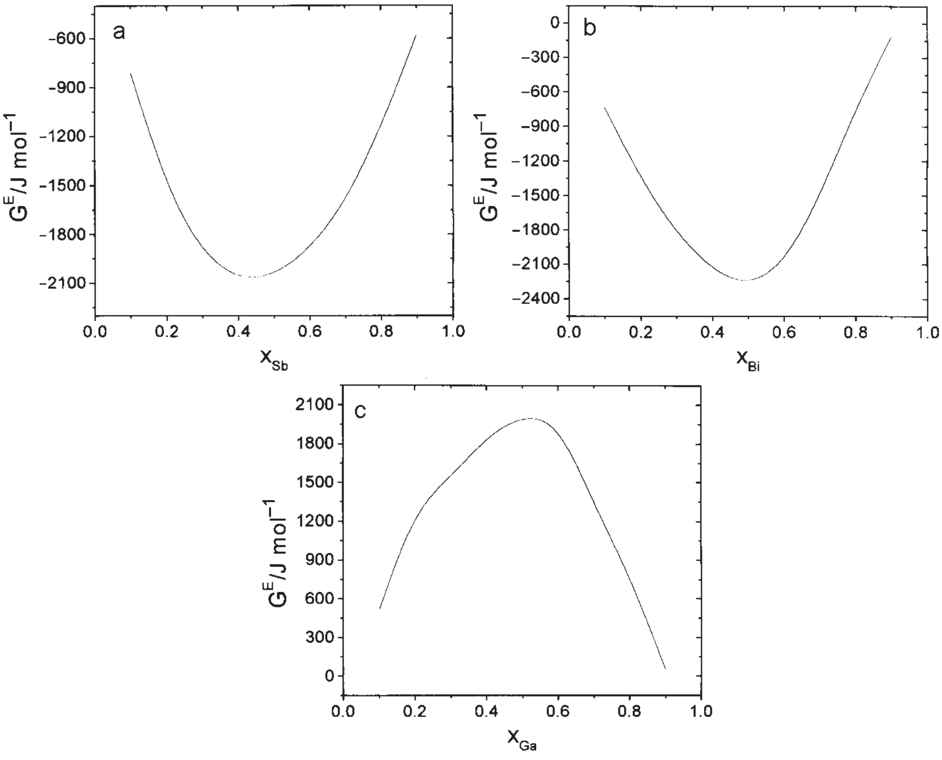

Fig. 7 The plots of G^E_{ij} *vs.* mole fraction x_i for three binary systems at a temperature of 1073 K (a – system Ga–Sb; b – system Sb–Bi; c – system Bi–Ga)

Concerning the application of the adequate thermodynamic predicting models for the determination of thermodynamic properties for Bi–GaSb system, first of all one should take a look at the constitutive three binaries. The plots of excess Gibbs energies for Ga–Sb, Sb–Bi and Bi–Ga at temperature 1073 K taken from references [7, 14, 1], respectively, are given in Fig. 7.

Binary regular – solution parameters and similarity coefficients for these systems at the investigated temperature, calculated according to Eq. (16) and Eqs (18–20), respectively, were taken from [22]. The values of the parameters are shown in Table 3, while the values of the similarity coefficients are $\xi_{Ga-Sb}=0.989$, $\xi_{Sb-Bi}=0.010$ and $\xi_{Bi-Ga}=0.498$.

Table 3 Binary regular-solution parameters for Ga–Sb, Sb–Bi and Bi–Ga binaries at 1073 K

Parameter	Ga–Sb	Sb–Bi	Bi–Ga
A^0_{ij}	–8414.89	–9111.98	8322.73
A^1_{ij}	–2079.99	–1135.14	551.75
A^2_{ij}	840.02	6906.7	–7464.84
A^3_{ij}	778.55	–5050.54	4361.18

Based on these starting data, calculations were carried out according to different predicting methods for all alloys in the investigated system Bi–GaSb at a temperature of 1073 K. The results of thermodynamic predictions according to the models of Kohler [32], Muggianu [33], Toop [34], Hillert [28] and Chou [29] are given in Table 4, the graphical representation is shown in Fig. 8.

Table 4 Integral excess Gibbs free energies G^E (in J mol^{-1}), for the Bi–GaSb system at 1073 K calculated by different predicting methods

Alloy	Kohler	Muggianu	Toop	Hillert	Chou
			G^E/J mol^{-1}		
L0	0	0	0	0	0
L1	55	55	55	60	89
L2	183	179	201	197	280
L3	70	–28	94	–45	103
L4	–517	–553	–515	–573	–410
L5	–1129	–1124	–1065	–1066	–1078
L6	–1900	–1789	–1648	–1672	–1835
L7	–2104	–2104	–2104	–2104	–2104

Good mutual agreement is noticed between the results of different applied thermodynamic predicting models, as can be noticed in the graphical representation shown in Fig. 8.

In order to compare the results of the thermodynamic predictions with the obtained experimental data at 1073 K, partial thermodynamic quantities for bismuth were calculated, based on the integral excess Gibbs energies determined from Kohler, Muggianu, Toop, Hillert and Chou results and shown in Table 5.

Finally, the comparison between experimentally obtained and predicted results could be made, at 1073 K. The graphic interpretation of such a comparison, for the example of the dependence of bismuth activity coefficient logarithm on composition, is given in Fig. 9.

Table 5 The calculated values for bismuth partial thermodynamic quantities from the predicted results

Alloy	Kohler		Muggianu		Toop		Hillert		Chou	
	a_{Bi}	γ_{Bi}	a_{Bi}	γ_{Bi}	a_{Bi}	γ_{Bi}	a_{Bi}	γ_{Bi}	a_{Bi}	γ_{Bi}
L0	1	1	1	1	1	1	1	1	1	1
L1	0.981	1.001	0.983	1.003	0.982	1.002	0.985	1.005	0.985	1.005
L2	0.910	1.011	0.915	1.017	0.914	1.016	0.919	1.022	0.918	1.020
L3	0.749	1.070	0.739	1.056	0.746	1.065	0.735	1.049	0.749	1.071
L4	0.567	1.135	0.554	1.109	0.556	1.112	0.545	1.089	0.574	1.149
L5	0.352	1.175	0.345	1.149	0.349	1.164	0.343	1.143	0.358	1.192
L6	0.109	1.086	0.111	1.111	0.115	1.145	0.115	1.147	0.119	1.119
L7	0	–	0	–	0	–	0	–	0	–

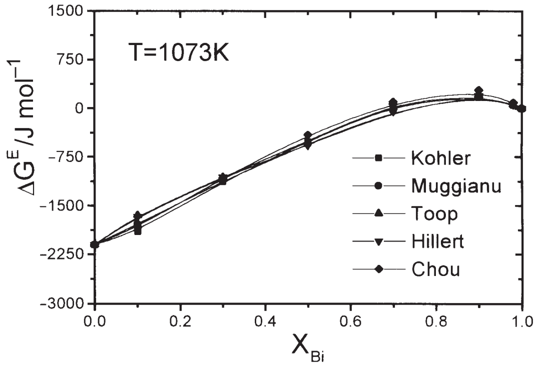

Fig. 8 Graphical representation of the predicted results

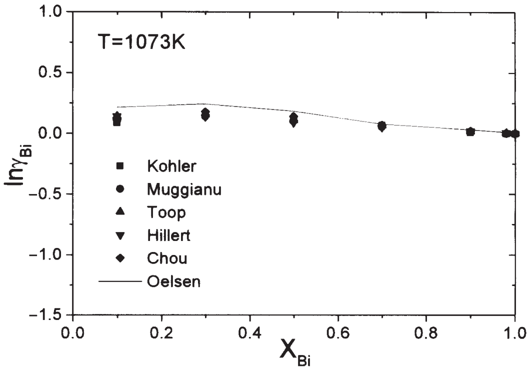

Fig. 9 Comparison between results for the dependence $\ln\gamma_{Bi}$–x_{Bi} at 1073 K

There is a slight deviation of experimental data comparing to the analytically obtained results for the Bi–GaSb thermodynamics. Since the investigated system is an asymmetric system, according to the plots of excess Gibbs energies for the constitutive binaries (Fig. 7) and values of the similarity coefficients [22], it could be expected that the asymmetric predicting models will give better results. So, if one takes the root mean square deviation corresponding to the Oelsen's $\ln\gamma_{Bi}$ values for each predicting model, i.e.

$$S=\frac{1}{N}\sqrt{\sum_{i=1}^{N}(\ln\gamma_{Bi_{(Predicted)\,i}}-\ln\gamma_{Bi_{(Experimental)\,i}})^2} \tag{21}$$

where $\ln\gamma_{Bi\ (Predicted)\ i}$ and $\ln\gamma_{Bi\ (Experimental)i)}$ represents the bismuth activity coefficient logarithm at a fixed composition *i* for a predicting model and the Oelsen's calorimetry, respectively, while *N* is the number of counting points, the results of such a calculation show that the *S* values for Kohler, Muggianu, Toop, Hillert and Chou models are 2.35; 2.47; 2.03; 2.38 and 1.85, respectively. Therefore, the thermodynamic properties of bismuth in the Bi–GaSb liquid alloys could be described mostly satisfactorily with the models of Chou and Toop.

Conclusions

The thermodynamic properties of the Bi–GaSb system were experimentally (Oelsen's calorimetry) and analytically (thermodynamic predicting models; Kohler, Muggianu, Toop, Hillert, Chou) determined and compared. The calculated results show agreement between data obtained by different models, as well as with experimental data. Also, phase diagram investigation confirmed the simple eutectic type of the investigated Bi–GaSb system. All of these results could be useful in further interpretation of the phenomena occurring in the ternary Bi–Ga–Sb system and in the compilation of the thermodynamic studies of III–V compounds-related materials at high temperatures.

* * *

The authors are grateful to Professor Jaroslav Šesták, Institute of Physics, Czech Academy of Sciences, Czech Republic, for his help and useful comments during the preparation of the paper.

References

1 I. Katayama, J. I. Nakayama, T. Ikura, Z. Kozuka and T. Iida, Mat. Trans. JIM, 34 (1993) 792.
2 I. Katayama, J. I. Nakayama, T. Ikura, T. Tanaka, Z. Kozuka and T. Iida, J. Non-Cryst. Sol., 156–158 (1993) 393.
3 J. Šestak, V. Šestakova, . ivković and D. ivković, Pure and Appl. Chem., 67 (1995) 1885.
4 I. Katayama, T. Ikura, K. Maki and T. Iida, Mat. Trans. JIM, 36 (1995) 41.
5 P. K. Liao, C. H. Su, T. Tung and R. F. Brebrick, CALPHAD, 6 (1982) 141.
6 L. Kaufman, J. Nell, K. Taylor and F. Hayes, CALPHAD, 5 (1981) 185.
7 I. Katayama, J. Nakayama, T. Nakai and Z. Kozuka, Trans. JIM, 28 (1987) 129.
8 C. Bergman, M. Laffite and Y. Muggianu, High Temp.-High Press, 6 (1974) 53.
9 T. J. Anderson, T. L. Aselage and L. F. Donaghey, J. Chem. Thermodyn., 15 (1983) 927.
10 T. Aselage, K. M. Chang and T. J. Anderson, CALPHAD, 9 (1985) 227.
11 R. C. Sharma, T. L. Ngai and Y. A. Chang, J. Electron. Mater., 16 (1987) 307.
12 I. A. Merzhanov, V. A. Geiderikh and V. I. Goryacheva, Zh. Fiz. Khim., 49 (1985) 874.
13 S. Ravindra Reddy, Mater. Sci. Eng., B20 (1993) 308.
14 R. Hultgren, P. D. Desai, D. T. Hawkins, M. Gleiser and K. Kelley, The Selected Values of the Thermodynamic Properties of Binary Alloys, ASM, Metals Park, OH 1973.
15 Y. Feutelais, G. Morgant, J. R. Didry and J. Schnitter, CALPHAD, 16 (1992) 111.
16 P. Taskinen and O. Teppo, Scand. J. Metall., 21 (1992) 138.
17 . ivković, D. ivković and J. Šesták, J. Therm. Anal., 43 (1995) 417.
18 B. Predel, M. Frebel and W. Gust, J. Less Comm. Met., 17 (1969) 391.
19 M. Gambino, J. P. Bros, F. Agersch and I. Ansara, Thermochim. Acta, 14 (1974) 305.
20 Z. Moser and K. Rzyman, Arch. Metall., 32 (1987) 3.
21 S. P. Yatsenko and V. N. Danilin, Neorgan. Mater., 4 (1968) 863 (in Russian).
22 D. ivković, . ivković and J. Šesták, CALPHAD, 23 (1999) 113.

23 D. Živković, Ž. Živković and B. Vučinić, J. Therm. Anal. Cal., 61 (2000) 263.
24 W. Oelsen and P. Zuhlke, Arch. Eisenhuttenwessen, 27 (1956) 743.
25 W. Oeslen, E. Schurmann, H. J. Weigt and O. Oelsen, Arch. Eisenhuttenwessen, 27 (1956) 487.
26 W. Oelsen, F. Bieret and G. Schwabe, Arch. Eisenhuttenwessen, 27 (1956) 607.
27 D. Živković, Ž. Živković and J. Šesták, Thermochim. Acta, 230 (1993) 77.
28 M. Hillert, CALPHAD, 4 (1980) 1.
29 K. C. Chou, CALPHAD, 19 (1995) 315.
30 K. C. Chou, W. C. Li, F. Li and M. He, CALPHAD, 20 (1996) 395.
31 D. Živković, Ž. Živković and Y. H. Liu, J. Alloy. Comp., 265 (1998) 176.
32 F. Kohler, Monatsch Chem., 91 (1960) 738.
33 Y. M. Muggianu, M. Gambino and J. P. Bross, J. Chimie Physique, 72 (1975) 83.
34 G. W. Toop, Trans. Met. Soc. AIME, 233 (1965) 850.
35 N. I. Gannina, A. M. Zaharov and L. A. Oleničeva, Phase diagrams of the metallic systems, Issue XXX, Part II, Metallurgia, Moscow 1986, p. 369 (in Russian).